Irreversible deposition of extended objects with diffusional relaxation on discrete substrates

I. Lončarević, Z.M. Jakšić, S.B. Vrhovac and Lj. Budinski-Petković

EDP
SCIENCES

Società Italiana
di Fisica

Springer

Regular Article

Irreversible deposition of extended objects with diffusional relaxation on discrete substrates

I. Lončarević[1], Z.M. Jakšić[2], S.B. Vrhovac[2,a], and Lj. Budinski-Petković[1]

[1] Faculty of Engineering, Trg D. Obradovića 6, Novi Sad 21000, Serbia
[2] Institute of Physics, P.O. Box 68, Zemun 11080, Belgrade, Serbia

Abstract. Random sequential adsorption with diffusional relaxation of extended objects both on a one-dimensional and planar triangular lattice is studied numerically by means of Monte Carlo simulations. We focus our attention on the behavior of the coverage $\theta(t)$ as a function of time. Our results indicate that the lattice dimensionality plays an important role in the present model. For deposition of k-mers on 1D lattice with diffusional relaxation, we found that the growth of the coverage $\theta(t)$ above the jamming limit to the closest packing limit θ_{CPL} is described by the pattern $\theta_{CPL} - \theta(t) \propto E_\beta[-(t/\tau)^\beta]$, where E_β denotes the Mittag-Leffler function of order $\beta \in (0,1)$. In the case of deposition of extended lattice shapes in 2D, we found that after the initial "jamming", a stretched exponential growth of the coverage $\theta(t)$ towards the closest packing limit θ_{CPL} occurs, i.e., $\theta_{CPL} - \theta(t) \propto \exp[-(t/\tau)^\beta]$. For both cases we observe that: (i) dependence of the relaxation time τ on the diffusion probability P_{dif} is consistent with a simple power-law, i.e., $\tau \propto P_{dif}^{-\delta}$; (ii) parameter β depends on the object size in 1D and on the particle shape in 2D.

1 Introduction

The Random Sequential Adsorption (RSA) model is a stochastic process in which objects of a specified shape are added sequentially to a D-dimensional volume at random positions with the condition that no trial particle can overlap. The adsorbed particles are permanently fixed at their spatial positions. Once an object is placed it affects the geometry of all later placements, so the dominant effect in RSA is the blocking of the available substrate volume. It allows to take into account the irreversibility of adsorption process and the volume exclusion effects. The RSA model studies were largely motivated by the surface deposition of micrometer-sized objects, such as colloid particles. It finds applications in many fields, ranging from surface physics to polymers, physical chemistry, biophysics and medicine [1–4].

The primary quantity of physical interest is the coverage $\theta(t)$, that is, the fraction of the substrate volume occupied by the adsorbed particles, as a function of time t. The deposition process ceases when all unoccupied spaces are smaller than the size of an adsorbed particle. The system is then jammed in a nonequilibrium disordered state for which the limiting (jamming) coverage θ_{jam} is less than

the corresponding density of closest packing. However, this picture is altered when diffusional relaxation is introduced [5–8]. Privman and Nielaba [5] have shown that the effect of added diffusion in the deposition process of dimers on the 1D lattice is to allow the *full* coverage via a $\propto t^{-1/2}$ power law at large times. The analysis is also extended to the 1D k-mers deposition [9]. In this case coverage $\theta(t)$ follows the mean-field law $\propto t^{1/(k-1)}$ for large times and $k \geq 3$, with possible logarithmic correction for $k = 3$.

The 2D deposition of extended objects with diffusional relaxation is of interest in protein deposition for example, where diffusional rearrangement of deposited particles is observable on the time scales of the deposition process [10]. Adsorption processes with diffusional relaxation are widely studied in 2D [2,11–14], but analytical solutions of this problem are very rare and usually limited to 1D systems [15]. These studies indicate a rich pattern of new effects as compared to 1D. Eisenberg and Baram [16] have found that the asymptotic coverage $\theta(\infty)$ is less than unity for the diffusional relaxation of crosses on a square lattice, whereas such a behavior is not observed in the case of squares, in which the full coverage is reached for an infinite system. In fact, in the case of RSA with diffusional relaxation of lattice hard squares

ᵃ e-mail: `vrhovac@ipb.ac.rs`

Table 1. The jamming coverages θ_{jam} for various shapes (x) of length $\ell^{(x)}$ on a triangular lattice. The colors (online only) are associated with the different order $n_s^{(x)}$ of symmetry axis. The estimated statistical errors are on the last given digits.

(x)	Shape	$n_s^{(x)}$	$\ell^{(x)}$	$\theta_{jam}^{(x)}$
(A)		2	1	0.9139
(B)		2		0.8362
(C)		1	2	0.8345
(D)		3		0.7970

in 2D the approach to the full coverage is given by the power law $\propto 1/\sqrt{t}$ [2,17,18]. Fusco et al. [12] computed the asymptotic coverage $\theta(\infty)$ in the presence of diffusion of k-mers up to $k = 5$ on a 2D square lattice, and found that the complete coverage is never attained for any value of k. The existence of dynamically frozen configurations slows down the late stage of deposition and does not allow the system to reach the complete coverage.

An important issue in 2D deposition is the influence of the shape of the adsorbed particle. Numerical simulations suggest that the size, aspect ratio and symmetry properties of the object do play a significant role in the processes of both irreversible and reversible deposition. The numerical analyses for the irreversible deposition of various object shapes and their mixtures on a triangular lattice [19,20] establish that the approach to the jamming limit follows the exponential law with the rate dependent mostly on the order of symmetry axis of the shape. In the reversible case of deposition on a triangular lattice [21], we have found that the coverage kinetics is severely slowed down with the increase of the order of symmetry of the shape.

No studies have been carried out along these lines for deposition with diffusional relaxation of extended objects onto a triangular lattice. In this work we first present the results of extensive numerical simulations of deposition with diffusional relaxation of k-mers on the 1D lattice. After that, we consider the kinetics of deposition of extended objects on a triangular lattice, accompanied by diffusional relaxation. The depositing objects are made by self-avoiding random walks on a 2D triangular lattice. On a triangular lattice objects with a symmetry axis of first, second, third and sixth order can be formed. Rotational symmetry of order n_s with respect to a particular axis perpendicular to the triangular lattice, means that rotation by an angle of $2\pi/n_s$ does not change the object. Some of these objects are shown in Table 1. We focus our attention on the intermediate- to long-time behavior of the coverage fraction $\theta(t)$. In particular, we try to find a universal functional type that describes the growth of the coverage $\theta(t)$ in the *whole* range above the jamming limit θ_{jam} in the best way.

The paper is organized as follows. Section 2 describes the details of the simulations. Approach of the coverage fraction $\theta(t)$ to the asymptotic coverage $\theta(\infty)$ is analyzed

in Sections 3 and 4. Finally, Section 5 contains some additional comments and final remarks.

2 Definition of the model and the simulation method

The simulations on the triangular lattice are explained in detail. Some details of the 1D simulations are pointed out afterwards.

In 2D, the Monte Carlo simulations are performed on a triangular lattice of size $L^2 = 120 \times 120$. In the simulations of deposition processes with diffusional relaxation the kinetics is governed by the diffusion to adsorption probability ratio [13,14]. At each Monte Carlo step adsorption is attempted with probability P_a and diffusion with probability P_{dif}. Since we are interested in the ratio P_{dif}/P_a, in order to save computer time, it is convenient to take the adsorption probability to be $P_a = 1$, i.e., to try an adsorption at each Monte Carlo step.

We start with an initially empty triangular lattice. Adsorption and diffusion processes perform simultaneously with corresponding probabilities. For each of these processes, a lattice site is chosen at random. In the case of adsorption, we attempt to place the object with the beginning at the selected site. If the selected site is unoccupied, one of the six possible orientations is chosen at random and deposition of the object is tried in that direction. We fix the beginning of the walk that makes the shape of length ℓ at the selected site and search whether all successive ℓ sites are unoccupied. If they are empty, we occupy these $\ell + 1$ sites and place the object. If, however, any of the ℓ sites are already occupied, the deposition attempt is rejected and the configuration remains unchanged. This scheme is usually called conventional or standard model of deposition. The other strategy to perform an RSA, where we check all possible directions from the selected site, is named the end-on model [19]. In the case of diffusion, which is possible only if there is a particle at the selected site, we choose one of the six possible directions at random, with equal probability, and try to move the selected object by one lattice spacing in that direction. The object is moved if it does not overlap with any of the previously deposited objects. If the attempted move is not possible, the object stays at its original position.

For 1D simulations, a lattice of size $L = 10^5$ was used. In the case of adsorption, we try to place the k-mer with the beginning at the selected site, i.e., we search whether k consecutive sites in a randomly chosen direction are unoccupied. If so, we place the object. Otherwise, we reject the deposition trial. When the attempted process is diffusion and if there is a beginning of a previously deposited object at the randomly selected site, we choose one of the two possible directions at random and try to move the selected k-mer for a lattice constant in that direction.

Periodic boundary conditions are used in all directions. The time t is counted by the number of adsorption attempts and scaled by the total number of lattice sites. The data are averaged over 100 independent runs for each

shape. The finite-size effects, which are generally weak, can be neglected for object sizes $<L/8$ [22].

3 RSA with diffusional relaxation on a one-dimensional lattice

Here we focus on the one dimensional lattice, and study the effects of diffusion on deposition of k-mers. Our main goal is to characterize, both qualitatively and quantitatively, the coverage dynamics of deposition process in the *whole* range above the jamming limit θ_{jam}.

In order to provide the best analytical approximation for the coverage fraction $\theta(t)$, we have probed the wide set of phenomenological fitting functions for relaxation processes in many complex disordered systems [23]. The best fit for the simulation's data was obtained by the Mittag-Leffler function. The corresponding fitting function is of the form

$$\theta(t) = \theta_{CPL} - \Delta\theta\, E_\beta(-(t/\tau)^\beta), \qquad (3.1)$$

where θ_{CPL}, $\Delta\theta$, τ, and β are the fitting parameters. E_β is the one-parameter Mittag-Leffler function of order β [24] defined by the series expansion

$$E_\beta\left[-(t/\tau)^\beta\right] = \sum_{n=0}^\infty \frac{(-(t/\tau)^\beta)^n}{\Gamma(1+\beta n)}. \qquad (3.2)$$

For $\beta = 1$, the Mittag-Leffler function with argument $-t/\tau$ reduces to a standard exponential decay, $E_1(-t/\tau) = \exp(-t/\tau)$. Parameter τ determines the characteristic time of the coverage evolution and β measures the rate of deposition process on this time scale. When the deposited k-mers are subject to diffusion, the coverage fraction approaches the closest packing limit θ_{CPL} for large times, $t \to \infty$; in the case of 1D lattice, $\theta_{CPL} = 1$ [5,8], because diffusion allows the formation of large gaps within which a fraction of deposition attempts can succeed.

When $0 < \beta < 1$, for small values of t, the Mittag-Leffler function is approximated by a stretched exponential form
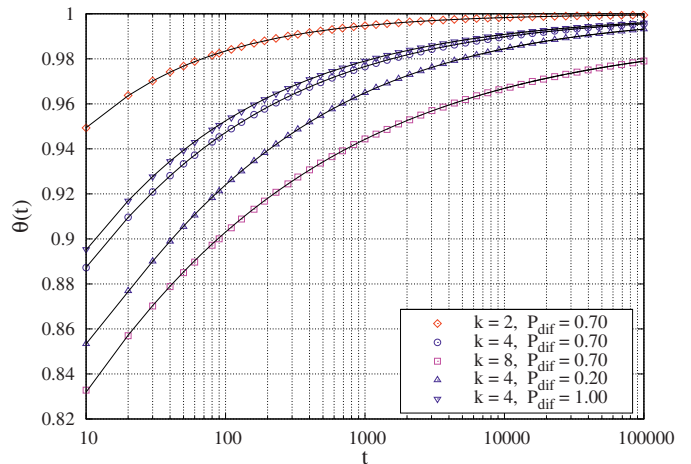
$$E_\beta\left[-(t/\tau)^\beta\right] \sim \exp\left[-\frac{1}{\Gamma(1+\beta)}(t/\tau)^\beta\right], \quad t \ll \tau. \ (3.3)$$

At long times the Mittag-Leffler function decays as a power law,

$$E_\beta\left[-(t/\tau)^\beta\right] \sim \frac{1}{\Gamma(1-\beta)}(t/\tau)^{-\beta}, \quad t \gg \tau. \qquad (3.4)$$

Using equations (3.1), (3.3) and (3.4) one obtains that the time-dependence of the coverage behaves as

$$\theta(t) \sim \theta_{CPL} - \Delta\theta\, \exp\left[-\frac{1}{\Gamma(1+\beta)}(t/\tau)^\beta\right], \quad t \ll \tau, \qquad (3.5)$$

Fig. 1. (Color online) Temporal behavior of the coverage $\theta(t)$ for deposition of k-mers: $k = 2$ ($\diamond$), $k = 4$ ($\bigcirc$, $\triangle$, $\triangledown$), and $k = 8$ ($\square$). The continuous curves are the Mittag-Lefler fits of equation (3.1). The results are for $P_{dif} = 0.2$ ($\triangle$), 0.7 ($\diamond$, $\bigcirc$, $\square$), and 1.0 ($\triangledown$).

and

$$\theta(t) \sim \theta_{CPL} - \Delta\theta\, \frac{1}{\Gamma(1-\beta)}(t/\tau)^{-\beta}, \quad t \gg \tau. \qquad (3.6)$$

Figure 1 shows the fit of equation (3.1) to some representative data ($k = 2$, 4, 8, and $P_{dif} = 0.2$, 0.7, 1.0). This indicates that the Mittag-Leffler function excellently describes the temporal evolution of the coverage fraction $\theta(t)$ in the *whole* post-jamming time range ($\theta(t) > \theta_{jam}$). To evaluate the existence of a power law at *late* times of deposition process, Figure 2 shows a comparisons of the Mittag-Leffler fit (3.1) and the power-law fit of empty area fraction $1 - \theta(t)$ in the case of dimers and 4-mers for two values of $P_{dif} = 0.1$, 0.5. The power-law fit is of the form

$$\theta(t) = \theta_{CPL} - \Delta\theta\, t^{-\beta}, \qquad (3.7)$$

where $\Delta\theta$ and β denote the fitting parameters that depend on the length of k-mer and on the diffusion probability P_{dif}. As it can be seen, at the very late times of the deposition process the plot of empty area fraction $1 - \theta(t)$ is nearly linear on a double logarithmic scale, indicating that the decay is consistent with a power law (3.7). This is in agreement with the previous results in 1D systems [5,8,12]. For the deposition of dimers ($k = 2$) we find that the closest packing limit $\theta_{CPL} = 1$ is approached according to the well-known $\sim 1/\sqrt{t}$ power-law [5,6]. It must be stressed that according to (3.6) the Mittag-Leffler pattern (3.1) is consistent with the power-law behavior for large times. However, Mittag-Leffler fit (3.1) precisely describes the adsorption process with diffusional relaxation on a wider time scale than the power-law (3.7).

In 1D, the main effect of diffusion is to increase the presence of large gaps at the expense of small gaps, which is particularly effective in the late stages of deposition. Hence, the power-law behavior is related to the coverage
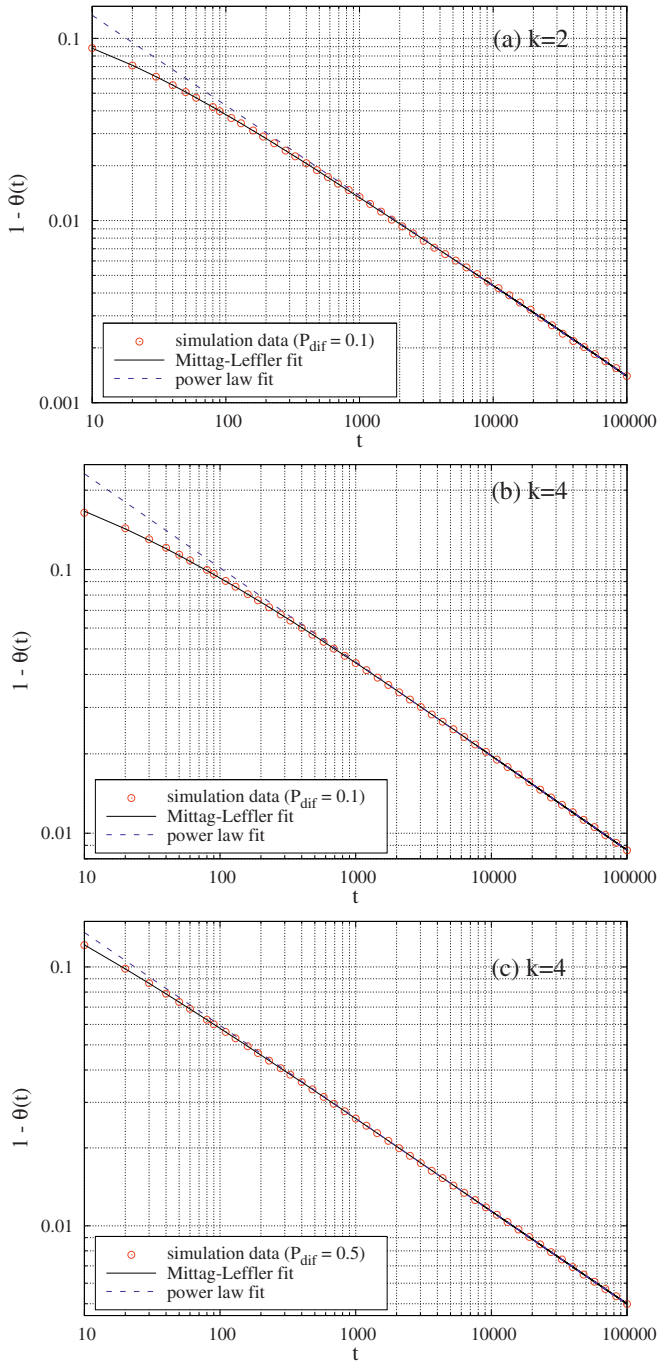
Fig. 2. (Color online) Temporal behavior of the coverage $\theta(t)$ for: (a) $k = 2$, $P_{dif} = 0.1$, (b) $k = 4$, $P_{dif} = 0.1$, and (c) $k = 4$, $P_{dif} = 0.5$. The continuous curves are the Mittag-Leffler fits of equation (3.1), and the dashed curves are the power-law fits of equation (3.7).

growth at large times by the process of hopping and recombination of small empty regions [5]. For the range of diffusion probabilities $P_{dif} = 0.1{-}1.0$, that we are dealing with in this work, the parameter β depends on the length of k-mers, but it is almost independent of the diffusion probability P_{dif}. The values for the parameter β obtained by least-square fits of the coverage $\theta(t)$ for
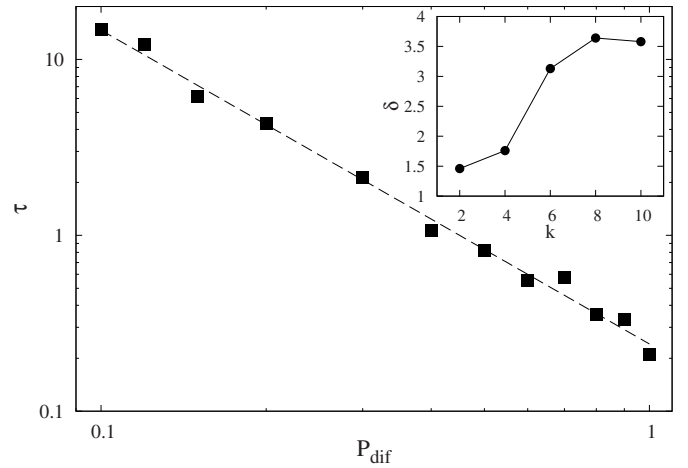
Fig. 3. Parameter τ of the Mittag-Leffler fit (3.1) vs. diffusion probability P_{dif} for $k = 4$. The dashed curve is the power-law fit of equation (3.8), with $\delta = 1.76 \pm 0.03$ and $A = 0.25 \pm 0.01$. The values of the parameter δ for $k = 2, 4, 6, 8$, and 10 are shown in the inset.

large t are roughly consistent with the mean-field relation $1 - \theta(t{-}\text{'large'}) \propto t^{1/(k-1)}$ for $k \geq 3$ [5,6]. Our simulation results for β exceed the mean-field values about 6% in the whole range of diffusion probability P_{dif} considered.

The dependence of the fitting parameter τ on the diffusion probability P_{dif} is shown in Figure 3 for the deposition of 4-mers. The first observation is the simple power-law dependence of τ on P_{dif}:

$$\tau = A \, P_{dif}^{-\delta}. \tag{3.8}$$

Similar plots are obtained for all k-mers, but with different slopes. The values of the parameter δ are obtained from these slopes and they are shown in the inset of Figure 3.

4 RSA with diffusional relaxation on a triangular lattice

In this section we report and discuss the numerical results regarding the effects of diffusion on deposition of extended objects on a two-dimensional triangular lattice. The simulations have been performed for a large number of various object shapes made by self-avoiding random walks on the lattice. Kinetics of the adsorption process with diffusional relaxation has been examined for all the shapes made by the self-avoiding walks of length $\ell = 1, 2$ and 3 and also for some objects of greater lengths. The set of the studied objects is similar to the one used in the simulations of the adsorption-desorption processes on the triangular lattice [21]. In Table 1 only a few representative objects are shown. Simulations of the deposition processes were performed for a wide range of diffusion probabilities, $P_{dif} = 0.01{-}1.0$.

In Figure 4 the time dependence of the coverage $\theta(t)$ in the case of irreversible deposition of object (D) is shown
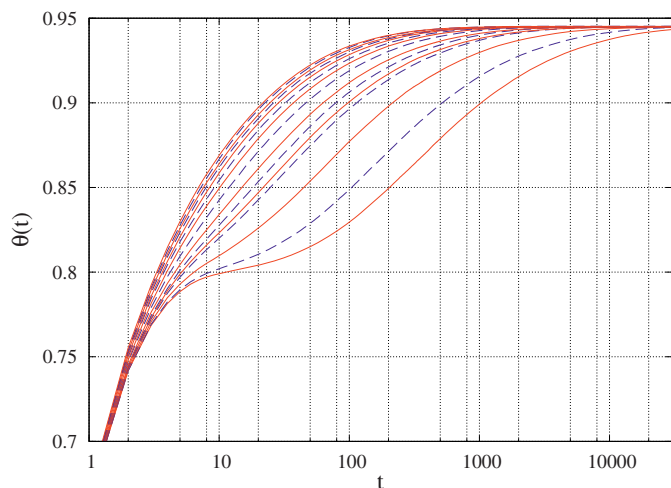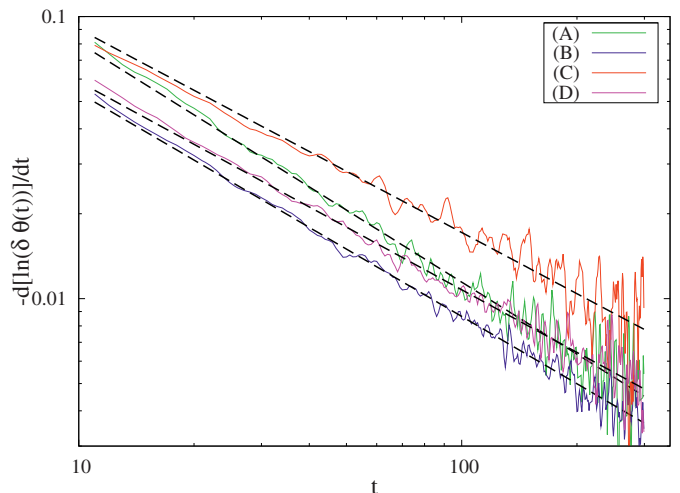
Fig. 4. (Color online) Temporal behavior of the coverage $\theta(t)$ for deposition of object (D) on a triangular lattice. The full (dashed) curves represent the adsorption process with diffusional relaxation for $P_{dif} = 1.0$, 0.90, 0.80, 0.70, 0.60, 0.50, 0.40, 0.30, 0.20, 0.15, 0.12, 0.10, 0.05, 0.02, and 0.01 from top to bottom.

Fig. 5. (Color online) Test for the presence of the stretched exponential law (4.1) in the time dependence of coverage $\theta(t)$ for objects (A) – green, (B) – blue, (C) – red, and (D) – violet (see, Tab. 1). The straight line sections of the curves show where the law holds. The dashed lines are the power-law fits of equation (4.5). All the results are for $P_{dif} = 1.0$.

for various values of diffusion probabilities P_{dif}. Numerical simulations for objects A, B, and C produce qualitatively similar results for the time evolution of the coverage $\theta(t)$. As it can be seen at coverages above the jamming limit ($\theta_{jam} = 0.7970$, for object (D)), the rearrangement of the objects on the lattice is more rapid and the maximum coverage is reached more quickly for greater diffusion probabilities. At very early times of the process, when the coverage is small, the adsorption process is dominant. With the growth of the coverage, diffusion becomes more important and at the late times additional adsorption events are possible only on the holes formed by the diffusion of the adsorbed objects. On a one-dimensional lattice, RSA with diffusional relaxation finally leads to a fully covered lattice. In two dimensions such processes lead to formation of large clusters of covered sites. After long enough times only few frozen defects, whose dimensions are less than the dimensions of the depositing objects, remain unoccupied [7].

We focus our interest on the temporal evolution of the coverage fraction $\theta(t)$ for various shapes. The large number of examined objects represents a good basis for testing various fitting functions and finding a universal functional type that describes the time coverage behavior $\theta(t)$ in the best way. As in the 1D case, we have tried a wide set of phenomenological fitting functions for the relaxation processes. The best agreement with our simulation data was obtained by the stretched exponential function. The fitting function we have used is of the form

$$\theta(t) = \theta_{CPL} - \Delta\theta \exp\left(-(t/\tau)^\beta\right), \qquad (4.1)$$

where θ_{CPL}, $\Delta\theta$, τ, and β are the fitting parameters. For given objects, the values of the maximum coverage θ_{CPL}, the parameter $\Delta\theta$ and the relaxation time τ depend on the diffusion probability P_{dif}.

In order to confirm the validity of the stretched exponential behavior of the coverage fraction $\theta(t)$, the following procedure was applied. Equation (4.1) can be written as

$$\delta\theta(t) = \Delta\theta \exp\left(-(t/\tau)^\beta\right), \qquad (4.2)$$

where $\delta\theta = \theta_{CPL} - \theta(t)$. The first derivative of $\delta\theta(t)$ (Eq. (4.2)) with respect to time t gives

$$\frac{d\,\delta\theta(t)}{dt} = -\Delta\theta \exp\left(-(t/\tau)^\beta\right) \frac{\beta}{\tau} \left(\frac{t}{\tau}\right)^{\beta-1}. \qquad (4.3)$$

From equation (4.3) one obtains

$$-\frac{1}{\delta\theta(t)} \frac{d\,\delta\theta(t)}{dt} = \frac{\beta}{\tau^\beta} t^{\beta-1}, \qquad (4.4)$$

i.e.,

$$-\frac{d}{dt}\left[\ln(\delta\theta(t))\right] = \frac{\beta}{\tau^\beta} t^{\beta-1}. \qquad (4.5)$$

Consequently, in the case of the stretched exponential behavior of the coverage fraction $\theta(t)$, a double logarithmic plot of the first time derivative of $\ln(\delta\theta(t))$ is a straight line.

The time derivatives of $\ln(\delta\theta(t))$ are calculated numerically from the simulation data. Representative examples of the double logarithmic plots of $-d\left[\ln(\delta\theta(t))\right]/dt$ are shown in Figure 5, for all the objects from Table 1 and for the diffusion probability $P_{dif} = 1.0$. One can see that these curves are straight lines in the whole post-jamming time range ($\theta(t) > \theta_{jam}$). The same is valid for all tested values of diffusion probabilities ($P_{dif} = 0.01-1.0$). This suggests that the relaxation of the coverage fraction $\theta(t)$ above the jamming limit to the closest packing limit θ_{CPL} on the two-dimensional triangular lattice is in fact given by the stretched exponential function of the form (4.1). Values of
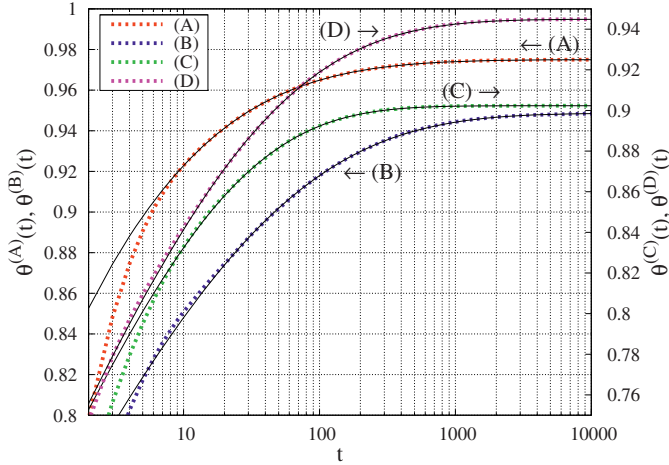
Fig. 6. (Color online) Temporal behavior of the coverage $\theta(t)$ for deposition of objects (A) – red, (B) – blue, (C) – green, and (D) – violet (see, Tab. 1) on a triangular lattice. The continuous curves are the stretched exponential fits of equation (4.1). All the results are for $P_{dif} = 0.30$. The arrows indicate that the graphs corresponding to objects (A) and (B) refer to the axis on the left-hand side. The remaining ones refer to the axis on the right-hand side.

the fitting parameters β and τ are determined from the power-law fit (4.5). The fitting values of the parameter $\Delta\theta$ are obtained for each pair (τ, β) by using the least-squares method.

In Figure 6 results of the numerical simulations are shown together with the stretched exponential fitting functions (4.1). The fitting parameters τ, β, and $\Delta\theta$ are obtained as described above. We can see that the stretched exponential fitting function shows an excellent agreement with the simulation results in the region above the jamming coverage. It should be noted that in this region the stretched exponential fits (4.1) of the simulation data give very high correlation coefficients ($\gtrsim 0.98$). In addition, the analysis of the time evolution of the coverage $\theta(t)$ above the jamming limit was also carried out by using the nonlinear fitting procedure, an implementation of the Nelder-Mead simplex algorithm [25], to minimize a nonlinear function of several variables. We have checked that both the fitting procedures give the same results for τ and β within the error bars. As the first procedure is easier to implement, it has been systematically used in the analysis of the results.

Dependence of the fitting parameter τ on the diffusion probability is shown on a double logarithmic scale in Figure 7. For all the objects these plots are straight lines approximately parallel to each other, indicating that the relaxation time τ is a simple power-law of the diffusion probability P_{dif}:

$$\tau = A\, P_{dif}^{-\gamma}, \qquad (4.6)$$

where A and γ are parameters that depend on the shape of depositing objects. The values of the exponent γ and parameter A are given in Table 2. One clearly observes that objects with similar aspect ratio, such as the objects
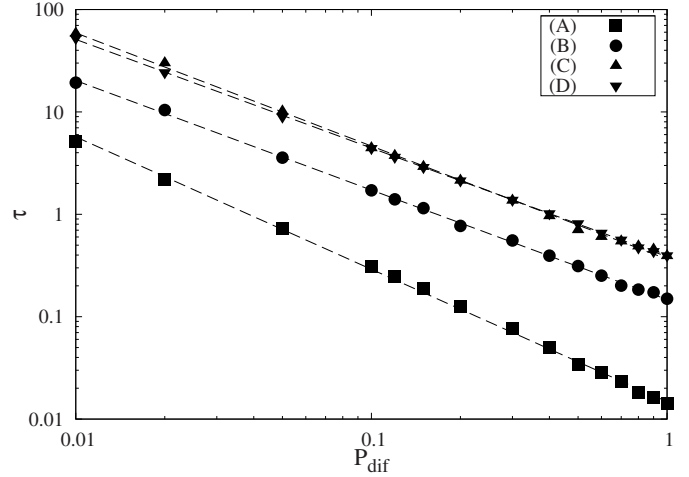
Fig. 7. Parameters τ of the fit (4.1) vs. diffusion probability P_{dif} for the shapes from Table 1. Squares, circles, triangles up, and triangles down correspond to the shapes (A), (B), (C) and (D) from Table 1, respectively. The dashed superimposed lines are the fits according to equation (4.6). The parameters of the fit (4.6) are reported in Table 2.

Table 2. Parameters A and γ determined using equation (4.6) for various shapes (x) of length $\ell^{(x)}$ on a triangular lattice. The typical statistical errors are estimated to the last given digits.

(x)	Shape	$n_s^{(x)}$	$\ell^{(x)}$	A	γ
(A)	●—●	2	1	0.0148	1.293
(B)	●—●—●	2		0.1471	1.069
(C)		1	2	0.3648	1.105
(D)		3		0.3856	1.061

C and D, have approximately equal relaxation times τ in the whole range of diffusion probability P_{dif} considered.

Interestingly, the fitting parameter β does not depend on the diffusion probability P_{dif}. The slopes of the straight lines in Figure 5, corresponding to the double logarithmic plots of $-d\left[\ln(\delta\theta(t))\right]/dt$ for various objects from Table 1, differ from object to object. From equation (4.5) it is obvious that these slopes are $\beta-1$ and the best fitting values of β are shown in Table 3 for all of the objects. It seems that β depends only on the shape and on the size of the object.

5 Final remarks

We have investigated numerically the kinetics of the deposition process of extended objects both on 1D and on the planar triangular lattice in the presence of diffusional relaxation. We focused on the time evolution of the coverage $\theta(t)$ in the whole post-jamming time range ($\theta(t) > \theta_{jam}$).

In one dimension, the growth of the coverage $\theta(t)$ above the jamming limit θ_{jam} to the closest packing limit $\theta_{CPL} \approx 1$ occurs via the Mittag-Leffler law (3.1), for all k-mers and for all values of diffusion probabilities P_{dif}. The characteristic timescale τ is found to decrease

Table 3. Parameter β determined using equation (4.5) for various shapes (x) of length $\ell^{(x)}$ on a triangular lattice. The typical statistical errors are estimated to the last given digits.

(x)	Shape	$n_s^{(x)}$	$\ell^{(x)}$	β
(A)		2	1	0.202
(B)		2		0.215
(C)		1	2	0.310
(D)		3		0.258

with the diffusion probability P_{dif} according to a power-law (3.8), $\tau \propto P_{dif}^{-\delta}$. We have also pointed out that the coverage fraction $\theta(t)$ at the late times of the deposition process approaches the closest packing limit according to a power-law (3.7) which is in agreement with the previous results [5,8,12]. It must be stressed that the Mittag-Leffler fit (3.1) accurately describes the adsorption process with diffusional relaxation on a wider time scale than the power-law (3.7).

We have also performed the numerical simulations of RSA with diffusional relaxation using the objects of different number of segments and rotational symmetries on a triangular lattice. The shapes are made by self-avoiding lattice steps. We have fitted the time dependences of the coverage fraction above the jamming limit θ_{jam} with the stretched-exponential function (4.1). This circumstance indicates that the lattice dimensionality plays an important role in the present model. We have also shown that the fitting parameter τ in equation (4.1) decreases algebraically with diffusion probability P_{dif}, as in equation (4.6). Two main conclusions can be drawn from the results (see, Fig. 6): (i) for the four different shapes, the maximum coverage is obtained for the most symmetric shape (D), and (ii) the maximum coverage for dimers is larger than that for 3-mers, i.e. the saturation coverage in 2D decreases with the length of k-mers. It was also shown that the dynamical behavior is severely slowed down with the increase of the length of the objects.

Both for the Mittag-Leffler (3.1) and the stretched-exponential fit (4.1), parameter β is characteristic of the particle size (1D) and the particle shape (2D). In one dimension, the corresponding exponents are found to be roughly in agreement with the mean-field results [5,6]. Our results in the case of diffusional relaxation on a triangular lattice suggest that the size, the aspect ratio and the symmetry properties of the object seem to have a significant influence on the parameter β.

Difference in the kinetics of the adsorption process with diffusional relaxation on one-dimensional and two-dimensional lattices is due to the orientational freedom of depositing objects. In 1D case the objects can adsorb only along the lattice and diffuse in two possible directions. On a triangular lattice there are six possible directions for adsorption and diffusion. On a two-dimensional lattice there is a greater number of possible orientations and an enhanced probability for the formation of frozen defects of blocked sites. Furthermore, the diffusion kinetics is affected by the number of motional degrees of freedom of the deposited objects.

References

1. J.W. Evans, Rev. Mod. Phys. **65**, 1281 (1993)
2. V. Privman, Colloids and Surfaces A **165**, 231 (2000)
3. B. Senger, J.C. Voegel, P. Schaaf, Colloids and Surfaces A **165**, 255 (2000)
4. A. Cadilhe, N.A.M. Araújo, V. Privman, J. Phys.: Condens. Matter **19**, 065124 (2007)
5. V. Privman, P. Nielaba, Europhys. Lett. **18**, 673 (1992)
6. V. Privman, M. Barma, J. Chem. Phys. **97**, 6714 (1992)
7. J.-S. Wang, P. Nielaba, V. Privman, Physica A **199**, 527 (1993)
8. J.W. Lee, B.H. Hong, J. Chem. Phys. **119**, 533 (2003)
9. P. Nielaba, V. Privman, J.S. Wang, J. Phys. A: Math. Gen. **23**, L1187 (1990)
10. J.J. Ramsden, J. Stat. Phys. **73**, 853 (1993)
11. G.G. Pereira, J.-S. Wang, Physica A **242**, 347 (1997)
12. C. Fusco, P. Gallo, A. Petri, M. Rovere, J. Chem. Phys. **114**, 7563 (2001)
13. Lj. Budinski-Petković, U. Kozmidis-Luburić, A. Mihailović, Physica A **293**, 339 (2001)
14. Lj. Budinski-Petković, T. Tošić, Physica A **329**, 350 (2003)
15. *Nonequilibrium Statistical Mechanics in One Dimension*, edited by V. Privman (Cambridge University Press, Cambridge, 1997)
16. E. Eisenberg, A. Baram, J. Phys. A **33**, 1729 (2000)
17. J.-S. Wang, P. Nielaba, V. Privman, Mod. Phys. Lett. B **7**, 189 (1993)
18. E. Eisenberg, A. Baram, Europhys. Lett. **44**, 168 (1998)
19. Lj. Budinski-Petković, U. Kozmidis-Luburić, Phys. Rev. E **56**, 6904 (1997)
20. Lj. Budinski-Petković, S.B. Vrhovac, I. Lončarević, Phys. Rev. E **78**, 061603 (2008)
21. Lj. Budinski-Petković, M. Petković, Z.M. Jakšić, S.B. Vrhovac, Phys. Rev. E **72**, 046118 (2005)
22. S.S. Manna, N.M. Švrakić, J. Phys. A: Math. Gen. **24**, L671 (1991)
23. R. Hilfer, J. Non-Cryst. Solids **305**, 122 (2002)
24. E.W. Weisstein, *Mittag-leffler function*, From MathWorld – A Wolfram Web Resource, http://mathworld.wolfram.com/Mittag-LefflerFunction.html
25. J.C. Lagarias, J.A. Reeds, M.H. Wright, P.E. Wright, SIAM Journal of Optimization **9**, 112 (1998)